Univerzita Karlova

Přírodovědecká fakulta

Studijní program: Geologie

Studijní obor: Geologie

Tatiana Tkáčiková

Analogové modelování procesů nad subdukčními zónami

Analog modeling of subduction zone processes

Bakalářská práce

Vedoucí bakalářské práce: prof. RNDr. Jiří Žák, Ph.D.
Konzultant bakalářské práce: RNDr. Jaroslava Hajná, Ph.D.

Praha, 2021

Prohlášení:

Prohlašuji, že jsem závěrečnou práci zpracovala samostatně pod vedením prof. RNDr. Jiřího Žáka, Ph.D. a že jsem uvedla všechny použité informační zdroje a literaturu. Tato práce ani její podstatná část nebyla předložena k získání jiného nebo stejného akademického titulu.

V Praze, 22.7.2021 Tatiana Tkáčiková

Acknowledgements

This thesis was written at the Institute of Geology and Paleontology, Faculty of Science, Charles University, and the experiments were performed in the Laboratory of Experimental Tectonics (funded from UNCE/SCI/006). I would love to express my sincere gratitude to my supervisor Jiří Žák, who took the time to help me create this thesis and whose classes inspired me to focus my study on geodynamics and plate tectonics. I would also like to thank Jaroslava Hajná for her help with setting up the experiments.

Contents

Abstract

Subduction zones, domains where oceanic lithosphere is subducted into the mantle beneath an overriding plate, are one of the most dynamic tectonic environments. A wide range of the long-lasting subduction-zone processes may be suitably reproduced and studied through analog modeling and thus may be directly observed in laboratory, though at time and length scales that differ fundamentally from nature. The main goals of this Bachelor thesis are first to provide an overview of large-scale architecture of subduction zones, to present an overview of the published analog experimental methods, and then to discuss the main outcomes of analog modeling of subduction zones and accretionary prisms. The thesis also summarizes the main mechanical parameters of materials used in the analog modeling. Furthermore, a set of simple experiments were performed, with the main goal to model formation of basalt-bearing mélanges during subduction of seamounts and volcanic belts that may occur on ocean floor and are commonly incorporated into accretionary wedges as dismembered Ocean Plate Stratigraphy (OPS).

Abstrakt

Subdukční zóny jsou jedním z nejdynamičtějších tektonických prostředí, kde se oceánská litosféra subdukuje pod nadložní desku do pláště. Pomocí analogového modelování lze vhodně studovat širokou škálu procesů subdukčních zón. Analogové modelování umožňuje reprodukovat komplikované a dlouhotrvající procesy, které tak lze pozorovat přímo v laboratoři, byť v kratších časových a délkových měřítkách než se odehrávají v přírodě. Hlavními cíli této bakalářské práce je nejprve poskytnout základní přehled architektury subdukčních zón, poskytnout přehled používaných analogových experimentálních metod a představit hlavní výsledky analogového modelování subdukčních zón a akrečních klínů. V práci jsou rovněž sumarizovány hlavní mechanické parametry modelovacích materiálů. V navazující části práce pak byly provedeny jednoduché analogové experimenty zaměřené na tvorbu melanží, které vznikají při subdukci podmořských hor a vulkanických pásů, jež se často tvoří topografické elevace na mořském dně. Tyto fragmenty spodní (subdukované) desky jsou pak často začleněny do akrečních klínů jako relikty tzv. stratigrafie oceánské desky (OPS – *Ocean Plate Stratigraphy*).

1 Introduction

Subduction zones at convergent plate margins are one of the most complex tectonic settings with frequent earthquakes, episodic but extensive volcanic activity, and dynamic surface processes. These areas represent unique deforming system between two lithospheric plates where material from the downgoing and overriding plates is dragged down into asthenosphere and further deep into Earth's mantle or exhumed back towards the surface. The subduction zones behave as a gigantic recycling system driving the plate tectonics and affect life and material transfer on the planet.

The dynamics of subduction zones has been extensively studied since the inception of the plate tectonic theory in the early 1960's through a variety of approaches, including field observations, geophysics, marine surveys, and the study of ophiolites. One of the most informative approaches to study subduction zones is scaled analog modeling that allows to directly observe the subduction processes under simplified conditions.

The main goals of this Bachelor thesis are (1) to provide a brief overview of overall architecture of subduction zones and, in particular, of geodynamic processes that drive plate tectonics and form structures associated with subduction, (2) review the analog modeling methods with a special reference to subduction zone processes, including material properties used in experimental modeling and overview of processes examined by analog modeling, and (3) perform new analog experiments that will try to reproduce one of the still enigmatic but widespread process, subduction of seamounts (seamount ridges/belts) and formation of mélanges.

2 Theoretical part: a brief overview of subduction zone processes

2.1 Driving forces of plate tectonics

Plate tectonics may be defined as the horizontal motion and mutual thermal and mechanical interactions of rigid lithospheric plates. In general, it is driven by two mechanisms: the “Down–Up” mantle upwelling and “Top–Down” oceanic slab-pull (Harper, 1975; Santosh, 2010).

The Down–Up mechanism takes place when a hot mantle plume originating from the core–mantle boundary (referred to as the D´´ layer) is partially melted and gains positive buoyancy, resulting in giant upwelling of hot mantle material up to the base of the lithosphere (Fig. 1). The upper portion of the plume spreads laterally beneath lithospheric plate and creates the plume head, which warms up the upper plate, causing the base of the lithosphere to melt while some of the mantle-derived magma may even rise to the Earth’s surface. The plume head also creates tensional forces and may lead to a complete break-up of the overlaying lithospheric plate (Chen et al., 2020).

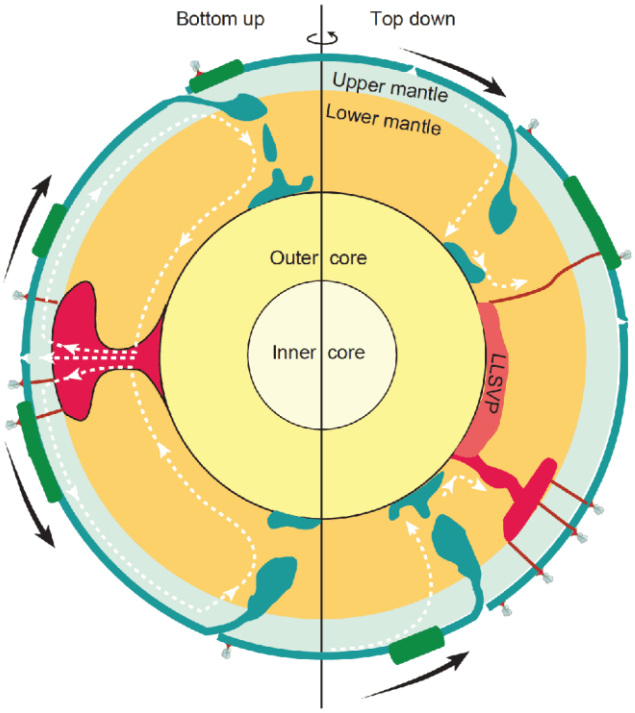

Figure 1. A simplified scheme of the *Down-Up* and *Top-Down* mechanisms of plate tectonics (Chen et al., 2020).

On the other hand, one of the key elements of plate tectonics is the subduction system, composed of subduction zones where relatively cold and thus negatively buoyant oceanic lithosphere sinks beneath the more buoyant continental lithosphere at the deep-sea trenches and is then incorporated into the mantle (Doglioni et al., 2007; Stern, 2002; Stern, 2004). This is referred to as the *Top–Down* mechanism (Fig. 1). What drives the oceanic plate into the subduction zone has long been debated, with the main forces acting on an oceanic lithosphere being the ridge-push, mantle traction at the base of the lithosphere, and slab-pull within the subduction zone. The latter, facilitated by dehydration and eclogitization, is now considered as the main driving force in modern-style plate tectonics (Forsyth and Uyeda, 1975; Chen et al., 2020). The eclogitization not only increases slab density but also slab dip and potentially the slab-breakoff depth (Huangfu et al., 2016).

The *Top–Down* mechanism is also a key mass transfer process that recycles the oceanic plate, including the overlying sedimentary layer, and thus modifies the composition of the mantle, affecting its chemical and physical properties and behavior (Ducea et al., 2009; Ducea et al., 2015; von Huene and Scholl, 1991). In the long run, subduction zones are responsible for destruction of ocean basins, crustal growth, shaping of active plate margins and are accountable for earthquakes, volcanism and other geohazards.

2.2 Anatomy of subduction zones and overview of the main geodynamic processes

Subduction zones have a complex architecture resulting from mechanical and thermal interactions of the subducting oceanic plate with the overriding oceanic or continental plate (Fig. 2). The age of seafloor that is about to descend at convergent margins ranges from approximately 170 Ma to 0 Ma with thickness of oceanic crust being relatively constant, ca. 6–7 km. The mean age of oceanic lithosphere when it arrives at a trench is ca. 100 Ma. As the lithosphere thickness increases through time, it becomes negatively buoyant with respect to the underlying asthenosphere, a cross-over point that occurs when the oceanic plate reaches an age of about 10–50 Ma (Stern, 2002). Cloetingh (1989) tried to calculate the relation between stress field and lithospheric rheology affecting passive margins. Their paper showed indications that after a certain period of time (>20 Ma), the oceanic lithosphere becomes too strong to deform by brittle faulting and it is thus very unlikely to be transferred into an active plate margin. In summary, old, dense oceanic lithosphere is more likely to sink (Cloos, 1993a), while too young and

buoyant lithosphere will tend to resist subduction.

Subduction zones are rather complex in terms of composition and structure (Fig. 1), the main components are briefly described below.

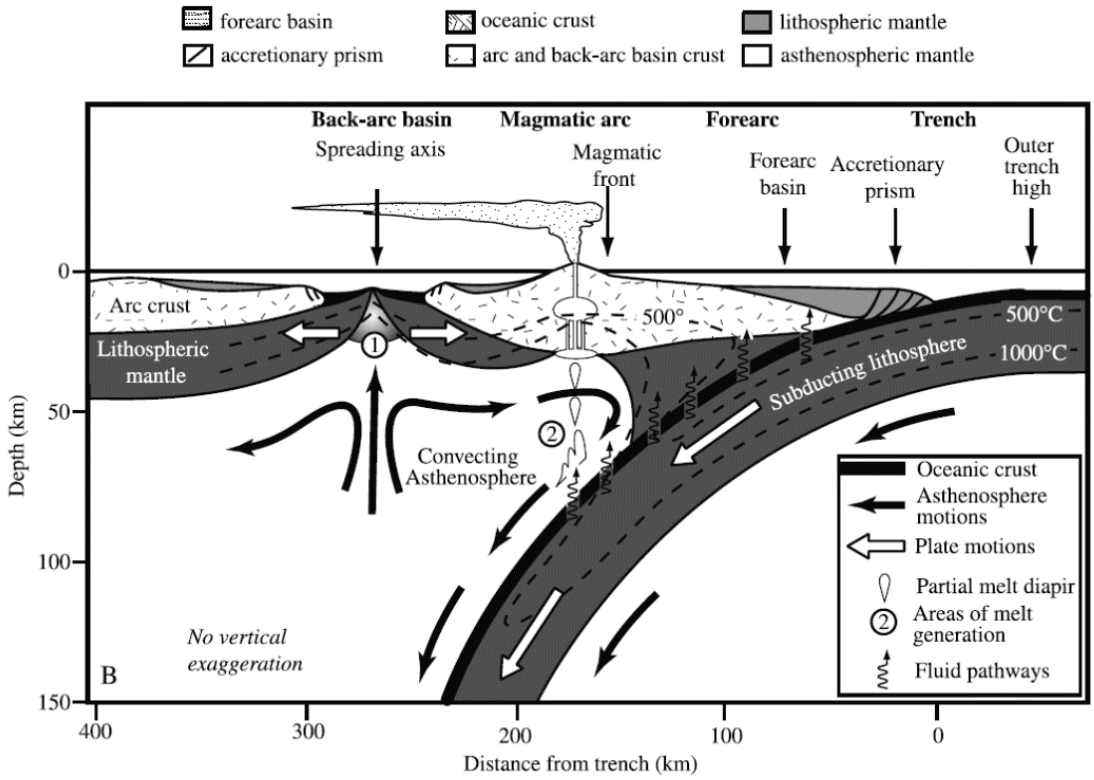

Figure 2. Idealized cross-section sowing the main components of subduction zones (Stern, 2002).

2.2.1 Trench

A deep-sea trench is a linear trough that develops where the oceanic plate bends and starts its descent into the mantle. The location of trench can change through time, either retreat seaward (slab roll-back) or advances toward the arc (Doglioni et al., 2007; Lallemand et al., 2008). Trench migration significantly affects subduction tectonics such as back-arc spreading or heat transport and mixing efficiency of mantle flow (Lallemand and Funiciello, 2009). Change in mantle conduction has a major impact on back-arc temperatures and volcanism, among others.

2.2.2 Fore-arc

The area between volcanic arc and trench is called the forearc region. It includes the trench itself, accretionary wedge, and forearc basins (Kearey et al., 2009). The same way as the trench, forearc progressively changes its structure and is a major site of deposition of arc-derived detritus.

2.2.3 The subduction channel

The dynamic interface between the subducting (lower) and overriding (upper) plate is referred to as the subduction channel (Agard et al., 2018). The subduction channel is often filled with extremely sheared subducted sediment. The subducted sediments may be viewed as deforming approximately as a Newtonian viscous fluid as they are dragged by the down-going lithosphere. Hence, the layer of sediment creates a zone across which a rate of shear deformation, compaction, and lithification is increased due to compression by the overriding plate. By contrast, the fluid pressure of seawater is pushing the sedimentary material back upwards. (Cloos and Shreve, 1988a) also postulated that only a certain amount of sediment can move downward past any particular point in subduction channel. When certain amount of sediment enters this particular point, the increased input of sediment thickens the channel, causing the opposite pressure gradient and the buoyancy of the sediment to take over, resulting in a zone of upflow and production of subduction mélange. The subduction mélange may capture blocks from early subducted blueschists and exhume them to shallow crustal levels (Cloos and Shreve, 1988a).

2.2.4 Magmatic arcs

The origin of arc magmas lies in the water contained in sea-floor sediment and the deeper sections of oceanic crust, which are carried down to depths (124 ± 38 km (Stern, 2002)) along the Wadati–Benioff zone. Here, hydrous minerals (part of the oceanic plate) release water due to the dehydration metamorphic reactions, triggering extensive melting of the overlying mantle wedge, and in some cases also the slab itself (Ducea et al., 2015). The corner flow of the asthenosphere in the mantle wedge also supplies the surface of subducted plate with heat. In particular, incorporation of hydrated sedimentary rocks into the asthenosphere has a massive impact on fertilization of mantle rocks (Wada et al., 2008). In turn, predominantly basaltic melts that rise up under the overriding plate (underplating) trigger melting of the upper plate. Mixing of mantle- and crustally-derived magmas then produces magmas of intermediate composition (Cloos and Shreve, 1988a). The ascending voluminous melts create a linear arc-shaped magmatic belt parallel to the trench called magmatic (volcanic) arc. Arc magmas are silica-dominated and calc-alkaline in the beginning with possible later evolution into shoshonitic (high-K) suites (Dickinson, 1975). In early stages of arc evolution, the high amount of water can enter asthenosphere producing magnesium-rich andesites called boninites, typically in forearc settings (Hickey and Frey, 1982).

2.2.5 Back-arc

Back-arc is a region that may evolve landward from magmatic arc on the overriding plate. The back-arc regions are divided into two types, extensional and compressional (Uyeda and Kanamori, 1979).

With shallow dip of subducted oceanic plate, the motion of the slab results in compression in the back-arc region of the overriding plate. Compression forms elevated topography with seismic and possibly also volcanic activity accompanied by horizontal shortening of the back-arc region.

In contrast, steep dip of the subducted plate results in decoupling and oceanward retreat of the trench, which causes the back-arc extension. In turn, extension of the back-arc region leads to formation of back-arc basins (Uyeda and Kanamori, 1979). Long-term extension in back-arc basins may lead to seafloor spreading (generating new oceanic crust) and also to trenchward migration of the volcanic arc axis (Kearey et al., 2009; Lallemand and Funiciello, 2009).

2.2.6 Implications for crustal growth

Topographic elevations (e.g., plateaus, ridges, seamounts, intraoceanic arcs) inside oceanic basins tend to accrete laterally onto the overriding lithosphere and in combination with magmatic arcs, they are thus involved in crustal growth (Cloos, 1993b). Closure of small oceanic basins could explain the repetitive absence of island-arc volcanism in the Wilson cycle and the emplacement of ophiolites (fragments of oceanic lithosphere) onto the overriding lithosphere (Cloetingh et al., 1989). The main external manifestation of accretion and magmatic arcs, that help geologists study plate tectonics, are ophiolites volcanism and earthquakes.

2.3 The Mariana and Chilean type subduction zones

The key effect of the ridge–trench distance, and thus of the age of oceanic lithosphere, on the slab dip during subduction is greatly exemplified in the Pacific Ocean basin. Here, two fundamentally different types of subduction zones occur on the western and eastern sides of the basin, referred to as the Mariana and Chilean type, respectively (Stern, 2002). (Jarrard, 1986) also found out that the strain regime in the overriding plate correlates with the age of the subducted lithosphere and absolute motion of overriding plate. He proposed seven strain classes between 1 - Mariana type, strongly extensional with weak coupling between plates and 7 - Chilean type strongly compressional with strong coupling between the two adjacent plates (Stern, 2002).

2.3.1 The Mariana type

The Mariana type subduction zones are characterized by slow subduction of old, dense lithosphere with relatively steep slab dip, generating volcanic island arcs with actively spreading back-arc basins accompanied by trench retreat (Fig. 3). Steep dip of the oceanic plate is a result of its higher density and thickness (greater with age) and the possible effect of seawater on the rheological properties of the down-going lithosphere. Dip of subduction also affects flow and rollback of asthenosphere in the mantle wedge generating back-arc spreading (Stern and Gerya, 2018) and trench retreat. Subduction of old and cold lithosphere is associated with less compressional seismic activity than young and fast subduction zones (Jarrard, 1986). Fast subduction of old and dense plates suppresses the geotherms significantly, thus it takes longer to heat the oceanic plate and, as a result, deepest earthquakes (up to the 660 km discontinuity).

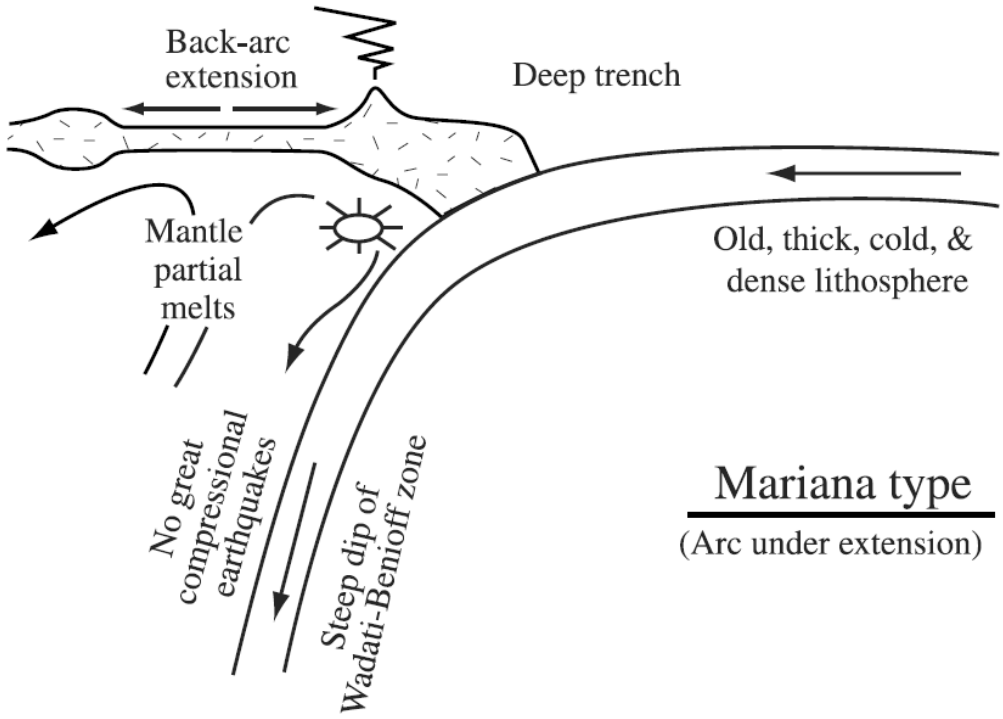

Figure 3. Schematic cross-section showing the Mariana-type subduction zone (Stern, 2002).

2.3.2 The Chilean type

The eastern side of the Pacific Ocean basin is delineated by the other, Chilean type subduction zone (Fig. 4). The young (20–30 Ma), thin, hot, and buoyant Nazca plate sinks under the South America continental lithosphere with a shallow dip of subduction. The Chilean type of

subduction is characterized by strong coupling, leading to shallow (<50 km) earthquakes, often of a large magnitude, accompanied by high stress and compressional deformation of the overriding plate with trench advance (Chen et al., 2020). Subduction dip also affects flow of the asthenosphere in the mantle wedge with shallow dips restricting this flow (Stern, 2002), leading to no back-arc extension.

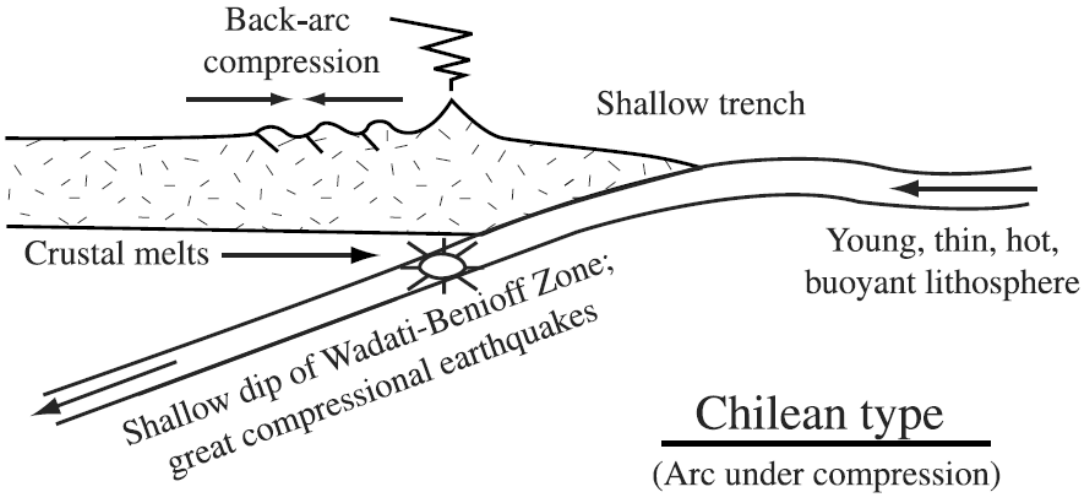

Figure 4. Schematic cross-section showing the Chilean type of subduction zone (Stern, 2002).

2.4 Accretionary vs. erosive active plate margins

Convergent plate margins may also be classified into two main groups, accretionary and erosive, based on whether material is added to or removed from the overriding plate (Clift and Vannucchi, 2004). Subduction erosion can occur at accretionary and erosive margins by erosion and collapse of the forearc wedge into the trench and by basal erosion by abrasion and hydrofracturing within the subduction channel. Subduction erosion also contributes to recycling of continental crust into mantle (Stern, 2011).

The Deep Sea Drilling Program (DSDP) and Ocean Drilling Program (ODP) in 1980s and 1990s revealed that accretion of sediment is a pointing feature in convergent margins (Clift, 2004). More than a half of all convergent margins on Earth are erosive rather than accretionary. It is important to say that during the existence of active convergent margins, accretionary margins may transfer into erosive and vice versa dependent on topology and sedimentary input from the hinterland (Simpson, 2010). The steepness of slope is directly proportional to speed of convergence and basal friction (Clift, 2004).

Active convergent margins with erosional dominance are favored in regions where convergence rate exceeds 6 cm/year. The high topography collides with the continental margin, scraping part of continental crust with it. Erosive margins are commonly associated with trench retreat. If we take the amount of sediment that enters the subduction channel, slow convergence will cause melting of enormous amount of material. Long-term erosion rates are more likely controlled by periodic collisions of topographic ridges with the trench (Clift, 2004).

Accretionary margins preferentially occur in regions with slower plate convergence, approximately 7.6 cm/year and less and with the trench sedimentary thickness >1 km. Accretion happens when the sedimentary cover, mostly sourced from the continental interior or arc, of oceanic plate is either scrapped off into the trench axis, or is underplated into the wedge at greater depths (Clift, 2004).

2.5 Accretionary wedges

Accretionary wedges (prisms) are wedge-shaped, structurally and compositionally complex bodies that form between the trench and margin of the overriding plate (Silver et al., 1985). The accretionary wedges grow by deposition of slope cover, by offscraping of sediment over the top, and by underplating of sediment to the bottom of the wedge (Cloos and Shreve, 1988b). To understand the processes of accretionary prism growth and deformation, we should also consider which types of rocks compose accretionary prisms: they are usually a mixture of terrigenous (upper plate) and oceanic (lower plate) material.

The upper part of the wedge slope is mostly covered with terrigenous sand, silt, and mud deposits transported trenchward, laterally from lows down canyons, or arckward from trench axis (Cloos and Shreve, 1988b). Most of the upper-slope sedimentary deposits are sourced from the volcanic arc (Clift et al., 1998) and are deposited by turbidity currents, slumps, or slides (Cloos and Shreve, 1988b; Ogata et al., 2020). In contrast, thin sedimentary layers scratched off the ocean floor can be considered as fine-grained accumulates slowly sinking to the bottom of the ocean called pelagic sediment. Under the term pelagic sediment falls mostly calcareous (pteropods) and siliceous (radiolarians) skeletal remains combined with other kinds of planktonic flora and fauna (Hüneke and Henrich, 2011). Pelagic components undergo metamorphism within the wedge or subduction channel into chert-like radiolarites.

Moreover, the accretionary wedges may involve dismembered volcanic complexes that formed the oceanic plate, either MORB or IOB. Mid-ocean ridge basalts (MORB) form by melting the mantle peridotite at mid ocean ridges (Arndt, 2011). During movement of an oceanic

plate from the mid-ocean ridge to the trench, the oceanic plate may be by mantle plumes to generate seamounts. Seamounts are composed of Ocean Island Basalt (OIB), olivine-bearing lavas with subalkalic (tholeiitic) and alkalic compositions (Safonova et al., 2016; Suetsugu et al., 2013). Altogether, the MORB, OIB, and pelagic and finally terrigenous sediments define a succession that tracks the movement of the oceanic plate from ridge to trench, referred to as the Ocean Plate Stratigraphy or OPS (Kusky et al., 2013; Matsuda and Isozaki, 1991) (Fig. 5). The OPS is a common part of accretionary wedges, but is frequently dismembered to form the OPS mélange (Wakita, 2015).

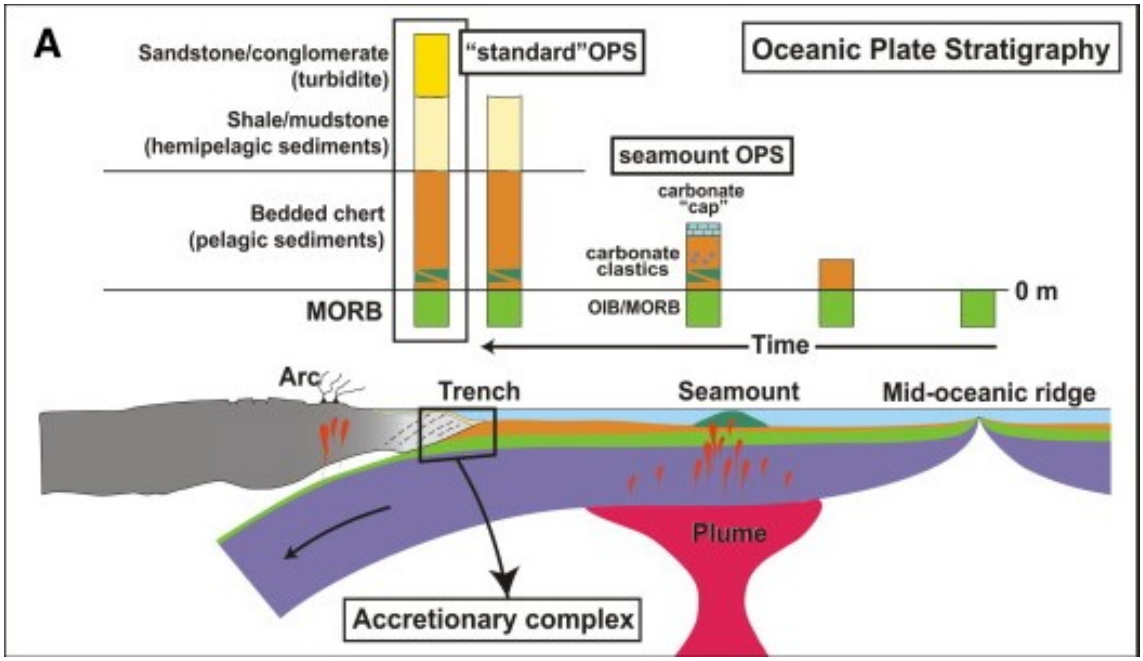

Figure 5. Diagram showing the concept of Ocean Plate Stratigraphy – OPS (Maruyama and Safonova, 2019).

The deformation of an accretionary wedge may be then viewed as a change in shape of sedimentary material in front of a moving bulldozer, controlled especially by the basal friction and material properties of the sediment. The layer of material in front of the bulldozer, now in subcritical state, will shorten and thicken until it reaches the so-called critical taper. If the wedge slope further increases (overcritical state), erosion of the wedge surface starts to reduce the wedge thickness. Accretion of sediment to the wedge and its internal deformation is accommodated by thrusting and folding. In-sequence thrust faults are characterized by a ramp and flat geometry with propagation towards the foreland. Usually after the in-sequence thrusting locks and is not capable of further accommodating the progressive shortening, the out-of-sequence thrusting leads to the formation of a new thrust plane cutting across the already deformed thrust stack (Morley, 1988).

2.6 Subduction mélanges

Mélanges can be defined as mappable units that consist of blocks of different size, origin, and metamorphic grade, formed by oceanic material, terrigenous sediment, or usually both, embedded in argillitic, sandy, or serpentinite matrix, or more rarely in carbonatic, evaporitic or volcanic matrix (Festa et al., 2010). Subduction mélanges form in subduction zone settings, often within the subduction channel or along megathrust surfaces, i.e., zones of intense shear deformation, or along the surface of the wedge (Fig. 6).

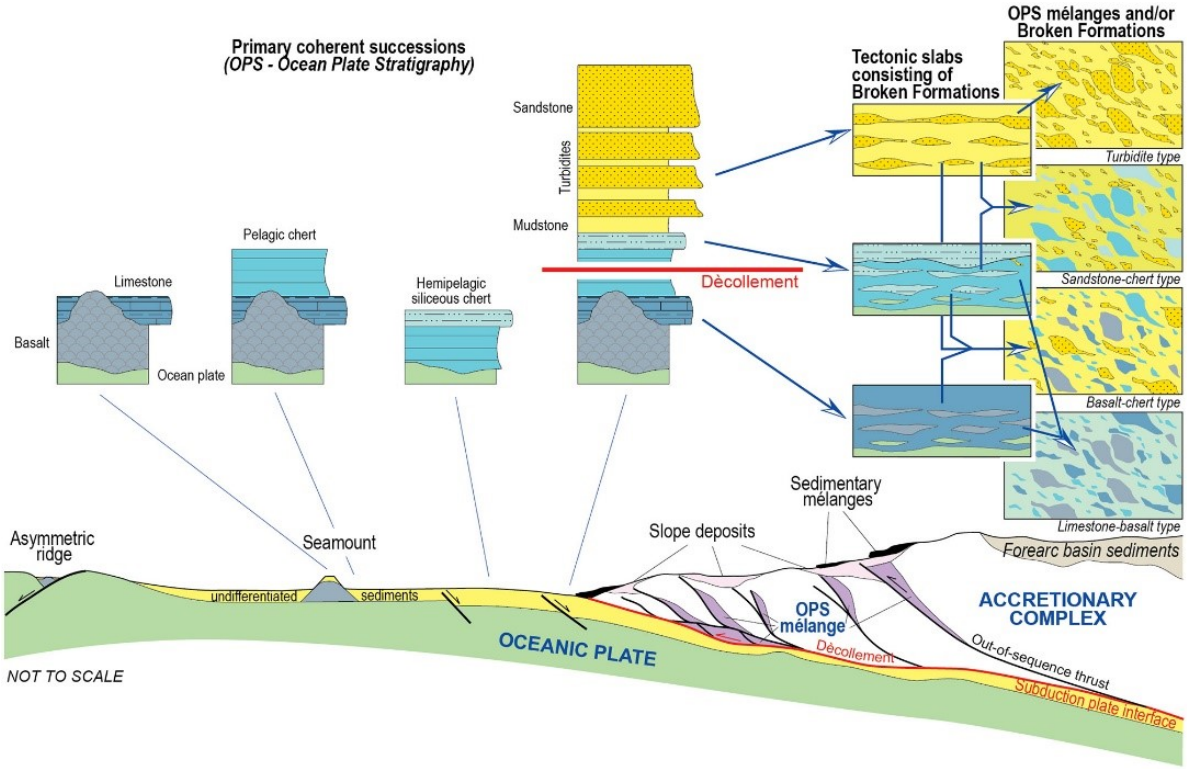

Figure 6. Diagram showing formation of subduction zone mélanges (Festa et al., 2019).

The main processes affecting mélanges are brittle and ductile deformation at shallow depths combined with high fluid pressure and related hydrofracturing (Raymond, 2019). Subduction mélanges may include various genetic types (Fig. 7). Mélanges developed by tectonic processes are called tectonic mélanges, very common in accretionary prisms. In contrast, sedimentary mélanges are associated with slump, gravity-flow or olistostromal activity in upper part of accretionary prisms linked with extension of continental slope. Diapiric mélanges form by intrusion of buoyant mobile material (serpentinite or mud) into the accretionary wedge, whereas polygenetic mélanges are commonly defined as produced by a combination of tectonic, sedimentary, and/or diapiric processes (Cloos and Shreve, 1988a; Festa et al., 2010; Festa et al.,

2019; Kusky et al., 2020).

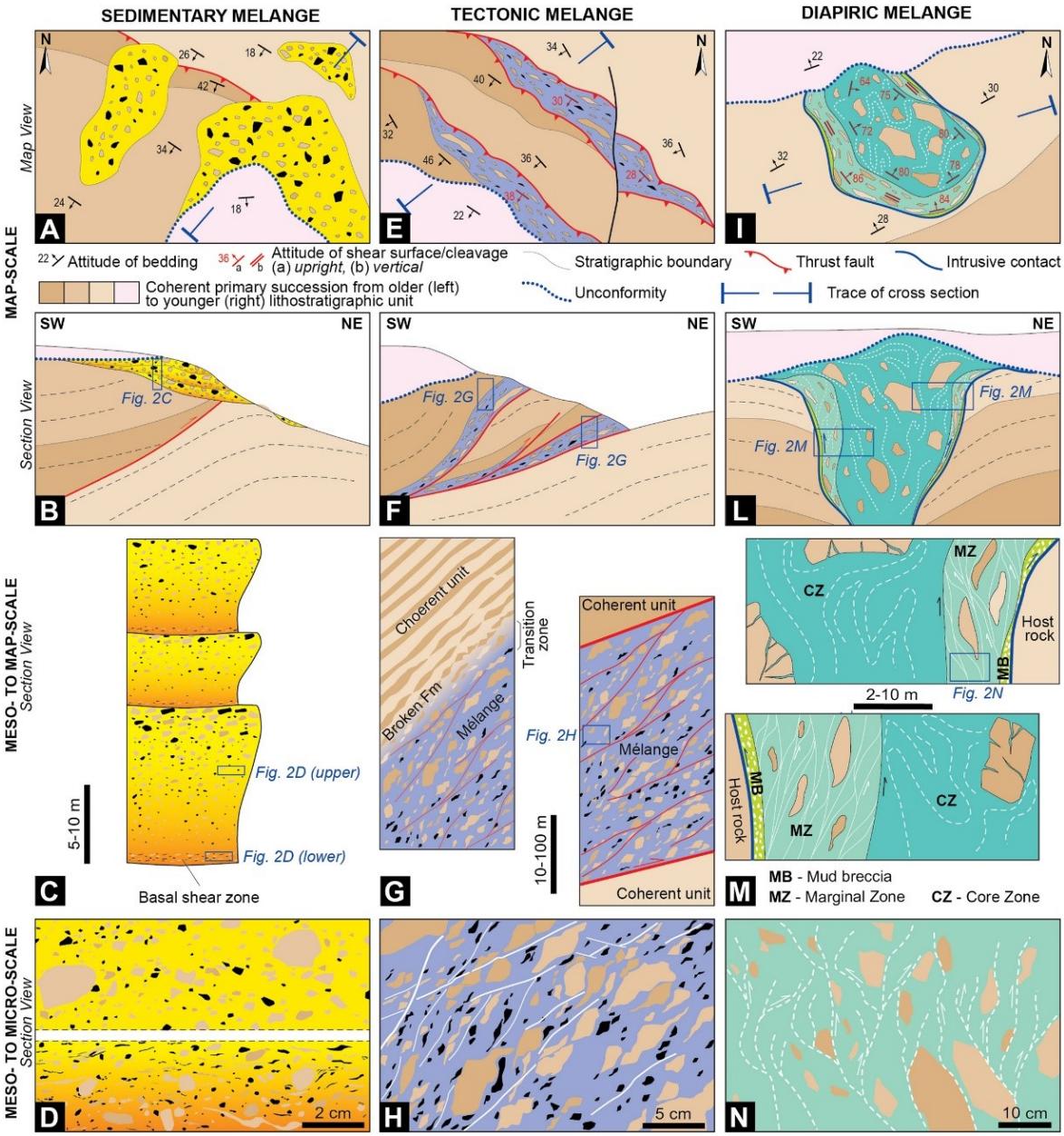

Figure 7. Diagram showing characteristic features of the main types of mélanges – sedimentary, tectonic, diapiric (Festa et al., 2019).

2.7 Seamount subduction

The subducting oceanic plate commonly exhibits a rugged topography with fault scarps, aseismic ridges, and seamount chains (Fig. 8). When entering a subduction zone, these topographic elevations cause significant deformation in the overriding plate, and in accretionary wedges in particular, and are also major features that cause tectonic erosion.

In detail, the seamount subduction at convergent plate margins undeniably leads to numerous dynamic processes, such as brittle faulting, ductile deformation, seismic activity, and mass-wasting that affect the topography and the rheology of the seamount, the upper plate surface, and the environment within the overriding plate along with deformation of the subduction channel at greater depths (e.g., (Ruh et al., 2016)). Entering of the seamount into the subduction system is accompanied with brittle deformation of the upper plate and with generation of overpressure landward of the seamount and underpressure trenchward of the seamount. The effect of these pressure changes onto the rheology of the overriding plate is one of the points in a long lasting debate, whether the seamount could produce large thrusts or whether it works as a mechanical barrier in seismic activity (Cloos and Shreve, 1996; Wang and Bilek, 2011).

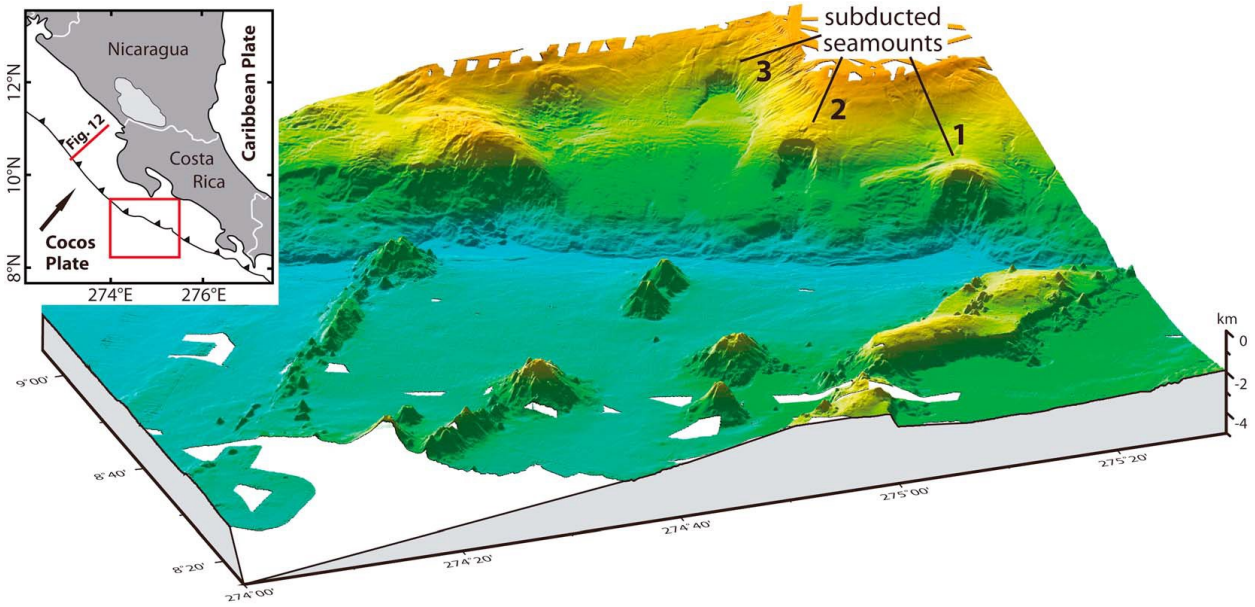

Figure 8. Three subducted seamounts in bathymetry of the Costa Rica active margin (Ruh et al., 2016).

The spacing and types of faults accompanying seamount subduction vary in relationship to the rheological and elastic properties of the seamount and the surrounding environment (e.g., total stress field, plate strength, strain weakening, etc.). The deformation of the seamount itself and style of its interaction with the overlying accretionary wedge is still the focus of vigorous research and it also varies in different types of the subduction zones. Wang and Bilek (2014) defined three types of seamount disintegration within the subduction channel: cutoff, sliding over, and breaking through. Moreover, the loose blocks, derived from the seamount either as pre-subduction debris or due to syn-subduction mechanical erosion, may be incorporated into the wedge or dragged down deeper into the subduction channel. The loose blocks may mix with the terrigenous siliciclastic matrix to form tectonic mélanges (e.g.,(Hajná et al., 2013)).

As to the surface manifestation during seamount collision, initially, a reentrant (V or U-shaped valley in the stress-shadow zone) forms behind the seamount (Fig. 8) and bulging deformation on the top of the seamount (Fig. 8) due to increasing mass (Ruh et al., 2016). This bulging and deformation lead to wedge slope collapse and submarine landsliding (Fig. 8), forming topographic scars (Fig.8) which are later filled with sediment (Hühnerbach et al., 2005). With continued subduction, topographic ridges and intervening piggy-back basins form atop of the subducted seamount.

3 Theoretical part: analog modeling

3.1 Analog modeling in tectonics: introduction and historical overview

Field measurements and observations in tectonics and geodynamics are often interpreted with the aid of experimental models that are performed in the laboratory conditions. These models are mostly based on numerical or analog techniques at smaller length and temporal scales, which may be combined when appropriate (Graveleau et al., 2012; Reber et al., 2020).

Analogue modeling is an experimental approach that uses simple physical models performed in the laboratory conditions to interpret geological and geodynamic processes and their evolution in space and time. Although the experimental models are rather simplified as compared to natural conditions, laboratory experiments have contributed greatly to our understanding of the development of a variety of geological structures. Analog modeling provides an opportunity to reconstruct geological processes that are not possible to observe directly in nature for they occur below the Earth's surface (e.g., magma or salt intrusions into the crust, processes within subduction zones) or that take a long geological time to form such as folding or other tectonic deformations (Buiter, 2012; Graveleau et al., 2012; Wang et al., 2021).

The history of analog modeling dates back to the beginning of the 19th century when a Scottish geologist Sir James Hall tried to explain the origin of folds. He used layered pieces of cloth, which were compressed by wooden boards. It was a successful set of experiments that formed folds resembling those observed in nature (Graveleau et al., 2012; Reber et al., 2020). Physical modeling then progressed significantly from layers of cloth to more suitable materials such as sand, clay, iron strings, and water. Experimental models became more elaborate and covered increasingly more complex natural processes. In 1878, Gabriel Auguste Daubrée modified the original Hall's model by adding colored wax in an attempt to model folding prior to faulting, essentially what could be considered as the first model of an accretionary wedge (Graveleau et al., 2012). Next, Henry Cadell studied mountain building processes in 1888 (thrust faulting) and was one of the first to address the problem of scaling (Reber et al., 2020). Subsequently, since the beginning of 20th century, the study of mountain building and geodynamics has expanded enormously with deeper understanding of observed systems, from folding to thrust faulting, fracturing, orogenesis, mountain building, and with the inception of the plate tectonics, models of large-scale processes became common (e.g., subduction, plate

tectonics, diapirism, etc.; (Schellart and Strak, 2016). Over the last 40 years, experimental modeling also converted from purely qualitative models, searching for the similarities between laboratory models and real situations, to quantitative studies of progressive deformation (Graveleau et al., 2012).

Since the very beginning of analog models, the two key aspects have appeared to warrant successful simulation of the geological processes in question: first, considering proper scaling between the analog model and the nature and, second, choosing convenient materials that will suitably replicate the nature.

3.1.1 Scaling

The scaling theory was introduced and elaborated by a pioneering work of Hubbert (1937) and involves geometric, kinematic, and dynamic similarity between natural process/structure and the physical model, allowing quantitative understanding of geodynamic processes in question (Schellart and Strak, 2016). The principle of the scaling theory is that the ratios between the corresponding parameters (e.g., length, density, viscosity) of the model and of the natural structure must be established to evaluate whether and to what extent the model corresponds to natural conditions. For example, geometric similarity means that angles are equal, and lengths are proportional as follows:

$$L_R = \frac{L_m}{L_n}$$

where L_R is the length ratio, L_m is length in the model, L_n is the length in natural structure.

3.1.2 An overview of materials used in the analog modeling

To perform a successful experimental model, we need to choose a proper variety of materials with similar rheological properties to those of the natural materials (minerals, rocks, or magmas (Reber et al., 2020). In comparison to nature, laboratory materials are always different, especially in terms of their stable chemical compositions, homogeneity, effect of fluids, and porosity. It is also important to consider that natural rocks are exposed to pressure and temperature conditions significantly different that those used in the physical models.

Dry sand, wet clay, wax, gelatin are the most commonly used materials for sandbox analog modeling (Buiter, 2012; Graveleau et al., 2012; Reber et al., 2020). The use of a particular material depends on the goal of the laboratory experiment. For modeling of upper-crustal processes, elastic materials capable of brittle deformation are used (e.g., clay, gelatin, wax, etc.), usually combined with granular materials (e.g., dry sand, glass beads, sand-powdered clay, etc.). For models of lower-crustal and mantle processes, Newtonian and non-Newtonian

fluids are used (Reber et al., 2020).

Tab. 1. Representative materials used in the analog modeling and their basic physical properties.

Material	Friction angle	Density (g/cm^3)	Cohesion (Pa)	Internal friction coefficient
Sand	25–45°	1.3–1.7	10–500	0.5–0.7
Micro beads	27–42°	0.85	50–250	0.4
Gelatin	-	1.3–1.4	-	-
Clay	45°	1.6–1.7	Depends on water content	0.6

3.1.2.1 Sand

Sand is dominantly used as a granular material in analog modeling experiments because it has suitable properties to reproduce brittle deformation. Its main advantage for modeling processes in the upper crust is that it produces localized shear zones similar to natural faults (Schellart and Strak, 2016).

Sand grains show distributed deformation and compaction followed by dilatation prior to failure. When an analog model reaches the yield stress, the elastic–plastic behavior of sand grains is expressed by frictional sliding within the system. The chemical, physical, and geometrical properties of sand grains (e.g., roughness, mineralogy, and grain size distribution) have a significant impact on the friction angle and shear strength during deformation (Reber et al., 2020).

3.1.2.2 Microbeads

Microbeads (glass microspheres) are a material that has been more recently used in addition to sand. Thanks to their ‘perfect’ sphericity, in contrast to more or less irregular sand grains, microbeads have a lower coefficient of internal friction than sand and thus are better suited to model crustal brittle behavior, and the décollement surfaces in particular. Microbeads are nowadays applied to low-friction scenarios and for layered mechanical stratigraphy. Mechanical properties of microbeads punctuate the resolution of faults development by decreasing the drag along experimental boundaries. In some models of salt diapirs, microbeads were covered with foam glass to create a smaller density contrast, yielding better results than when overburden was sand (Reber et al., 2020; Schellart and Strak, 2016).

3.1.2.3 Clay

As a visco-elastic material, clay is used to simulate inelastic deformations, which are modeled over a long period of time. It is widely used as an additional material in brittle modeling for its elasticity increase with strain rate while shear strength remains independent (Reber et al., 2020). Its mechanical and physical properties strongly depend on the of water content.

3.1.2.4 Gelatin

Gelatin as a visco-elastic material is typically used to model complex rheological behavior of the crust, lithosphere, and sub-lithospheric mantle. For its elastic brittle rheology, gelatin is commonly utilized in modeling of magma ascent and emplacement processes (Schellart and Strak, 2016). Unlike brittle material, gelatin's mechanical behavior depends on temperature, strain rate, composition, concentration, and pH. Thus it is a suitable material also to experimentally model tensile fracturing and earthquake processes (Reber et al., 2020).

3.1.3 Analogue modeling of accretionary wedges

As mentioned above, with the development of plate tectonics, experimental modeling applied to subduction zones and accretionary wedge dynamics has been a growing field of research for more than past 40 years. There are several main approaches to physically model the subduction zones and overlying wedges.

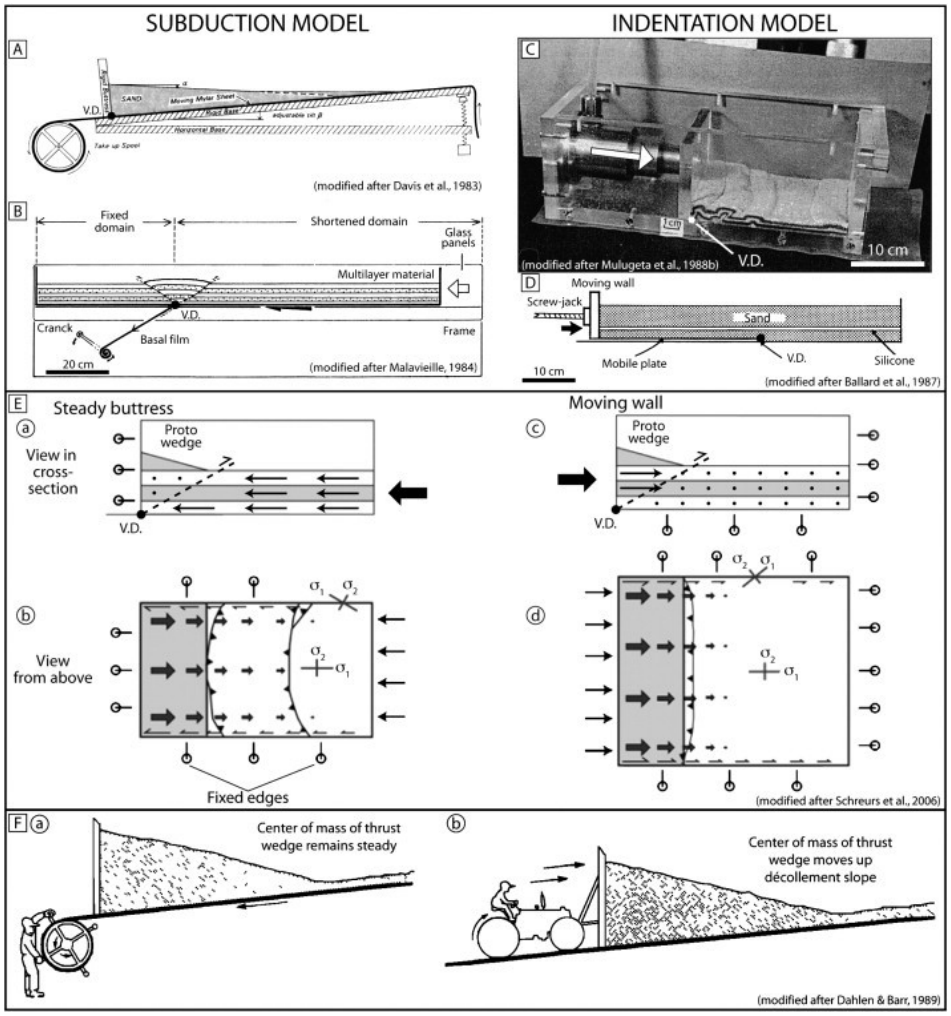

Figure 9. Different types of boundary conditions in sandbox modeling. A and B rolling the basal film, C and D moving the backstop (Graveleau et al., 2012).

The “sandbox” modeling technique is the most widely used to observe the growth and deformation of accretionary wedges. These experiments imitate plate convergence with a layered stack, mostly containing dry, cohesive granular materials, that is dragged by "subducting" plate (usually a moving or fixed sheet) and deformed against a rigid backstop (Graveleau et al., 2012) (Fig. 9). Laboratory models are usually performed under natural gravity field conditions, material physical properties (cohesion, viscosity, etc.) may be adapted in order to follow the scaling rule.

This Bc. thesis focuses on analog modeling of accretionary wedges and thus models of the most important processes are mentioned below.

3.1.3.1 Accretion and underplating

A number of analog experiments examined the processes of frontal accretion and offscraping of sediment at the toe of accretionary wedges, as well as development of internal wedge deformation, in particular in-sequence and out-of-sequence thrusts, décollements, and exhumation and associated normal faulting in the rear of accretionary wedges(Gutscher et al., 1998; Noda et al., 2020) (Fig. 10). The latter was mostly due to a process known as underplating whereby sediment that in not frontally accreted or offscraped enters the subduction zone. (Cowan and Silling, 1978) made a series of analog models that showed how the sediment that entered the subduction zone affects the critical taper and wedge kinematics through underplating. After underplating, the rear part of the wedge was thickened and started to increase the wedge slope, leading to exhumation of deeper portions of the wedge (Cowan and Silling, 1978).

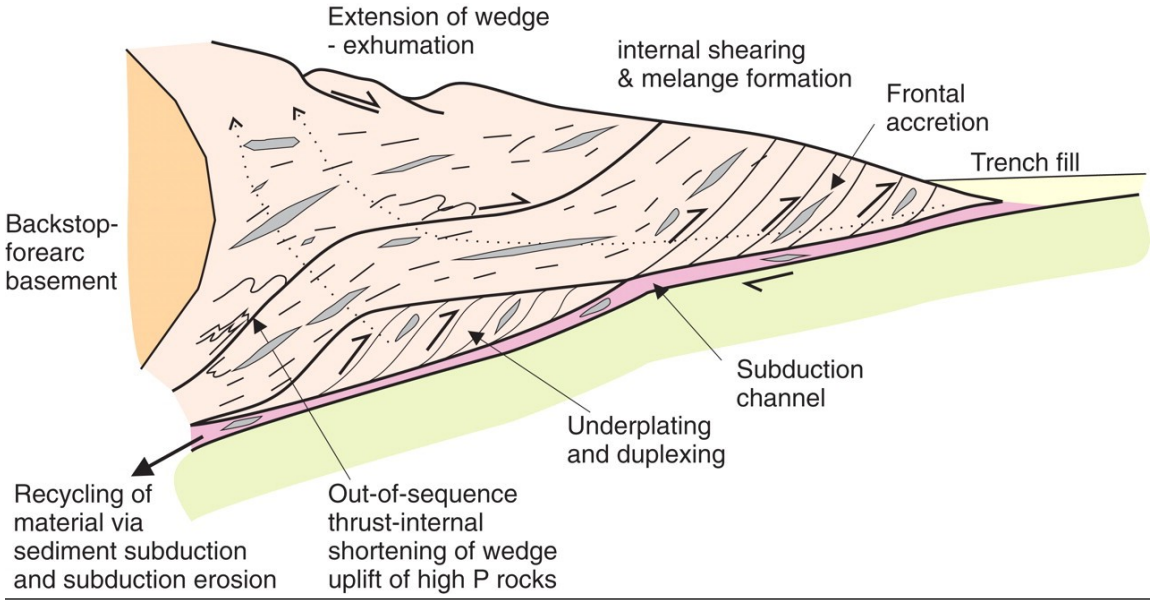

Figure 10. Illustration of main tectonic processes in accretionary wedges (Cawood et al., 2009).

3.1.3.2 Surface erosion of accretionary prism

Experimental modeling of accretionary wedges usually does not include erosion as a part of the experiment, though it is definitely significant in natural conditions. A few studies that examined the surface wedge erosion removed the material from the top surface by various means such vacuum cleaner or waterdrops simulating streams (Schellart and Strak, 2016). Generally, the amount of material that is eroded from a laboratory model usually equals to volume of material that enters the accretionary wedge, or the angle of wedge (usually 4–8°) is set in advance. Geometry and kinematics of erosional analog models suggests that erosion reduces the number of active thrust faults in an accretionary prism and therefore, prolongs the life of the active ones, reduces the width of the wedge, and contributes to reactivation of earlier formed structures and of out-of-sequence thrusts (Graveleau et al., 2012).

3.1.3.3 Seamounts entering subduction zone

Deformation of accretionary wedges caused by seamounts or volcanic ridges entering subduction zones has been well studied by analog and numerical studies (Dominguez et al., 1998; Noda et al., 2020). The seamounts, representing significant elevations on ocean floor, resist subduction and produce intense deformation of the overlaying soft wedge (Dominguez et al., 2000). Analog modeling successfully demonstrates the effect of seamount subduction and showed a variety of structures that develop in the deforming zone around the seamounts and involve uplift and subsidence, strike-slip faulting, fan-like fault network associated with backthrusts and out-of-sequence thrusting (Dominguez et al., 1998).

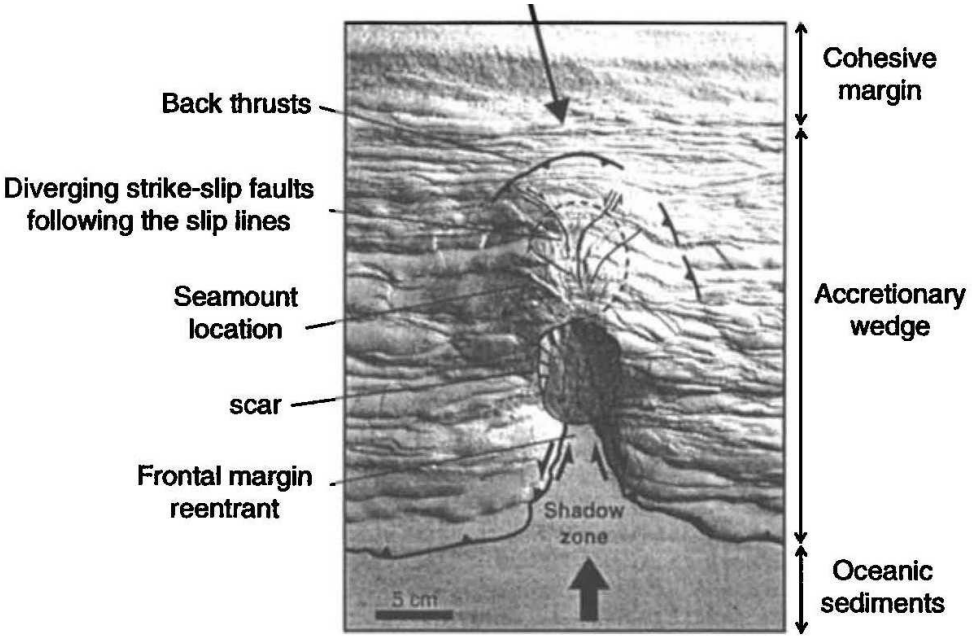

Figure 10. The main surface deformation features around subducting seamount (Dominguez et al., 2000).

4 Experimental part

4.1 Experimental apparatus

All experiments were performed in the Laboratory of Experimental Tectonics at the Institute of Geology and Paleontology, Charles University, Prague. The experimental apparatus is a sophisticated sandbox similar to those used to model a variety of subduction-zone processes (e.g., Graveleau et al., 2012). The deformation rig consists of plexi-glass sides, a polyvinyl-chloride (PVC) sheet loop put on a series of adjustable cylindrical hinges, a thin wooden plate mounted on an adjustable frame as a rigid backstop (allowing to change both the dip of the backstop and thus friction), and a motor and control unit (Fig. 12). The control unit is connected to PC and controlled by an in-house software. The internal dimensions of the experimental space are 40 × 20 × 250 cm (height, width, and length, respectively).

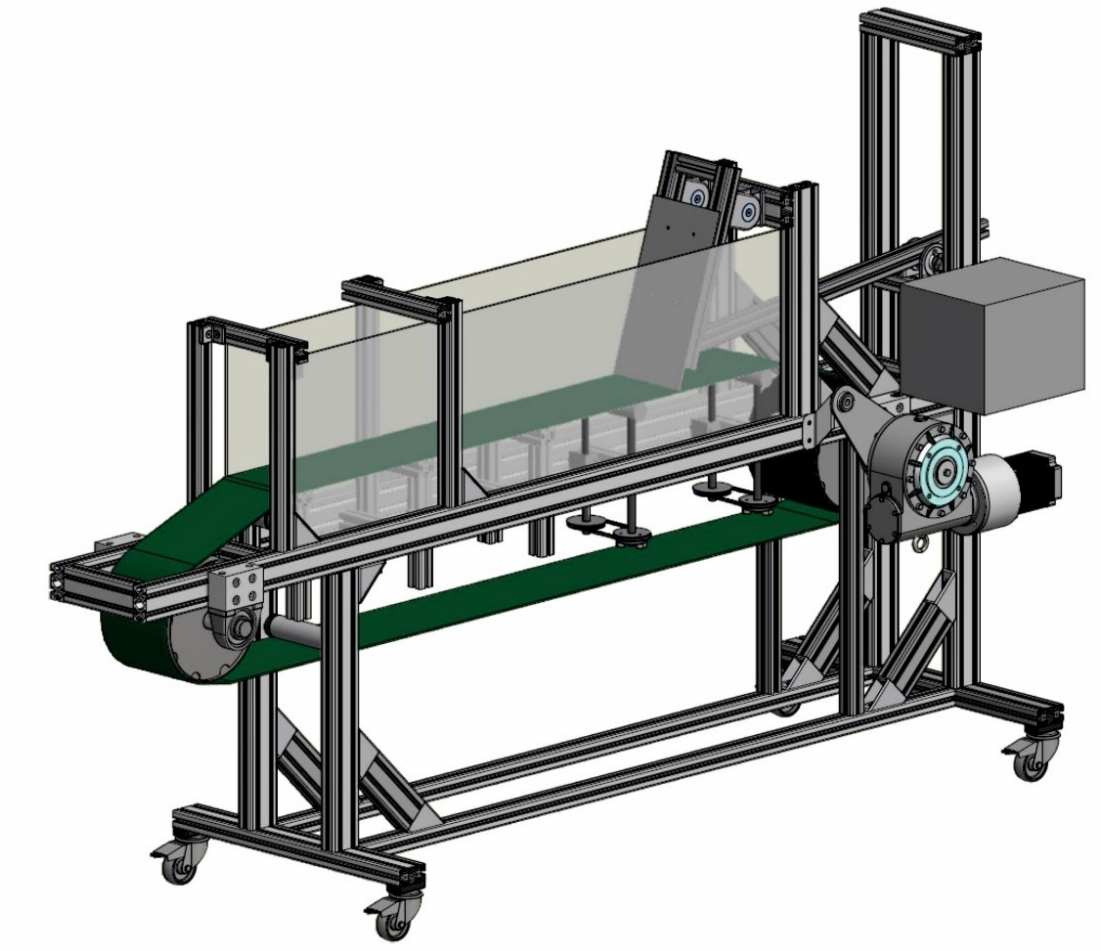

Figure 12. Scheme of the experimental apparatus used in the analog modeling (designed by O. Pačes for the Laboratory of Experimental Tectonics, Institute of Geology and Paleontology, Charles University, Prague).

4.2 Design of the experiments

As the main goal of the experiments was to model formation of mélanges during seamount subduction, the model consisted of two parts, representing an accretionary wedge and an off-shore seamount chains (volcanic ridges). The accretionary wedge was modeled using a dry, isotropic, virtually cohesionless aeolian quartz sand with 100–300 μm grain size, density $\rho = 1.6$ g/cm^3, and a coefficient of internal friction $\mu = 0.6$. Using a scaling factor of 10^{-5}, 1 cm of the model then represented approximately 1 km in nature. The seamount was modeled as a stack of pieces (blocks) of basalt (with 0.2–0.3 mm grain size and density $\rho = 2.9$ g/cm^3) to simulate thick debris aprons that are the main component of natural examples (e.g., (Wang et al., 2021)).

Two experiments were performed (referred to as the experiment 1 and 2) the former reproducing subduction of a single seamount and the latter subduction of several seamount chains (volcanic belts or ridges).

The first experiment was designed as a thin-sheet experiment, where four portions of sand, each of 256 g in weight but differing in color, were poured onto the PVC sheet to produce uniformly thick layers parallel to the surface of the "subducting oceanic plate" in front of the rigid backstop. The seamount (0 cm above the PVC sheet representing "seafloor") was placed as a stack of basalt blocks placed initially 20 cm from the backstop. Each layer had dimensions of 0.2 × 20 × 40 cm (thickness, width, and length, respectively). The rigid backstop had a moderate dip of 60° in the experiment. In front of the backstop, the dip of the "subducting oceanic plate" was 0°. The subduction zone inlet is represented in the experiment by a gap between the lower backstop edge and surface of the PVC sheet and was 1mm. The rate of PVC sheet motion ("subduction") was 0.01 cm/s in the experiment. The running experiment was captured every 30 s by a digital single-lens reflex (SLR) camera.

The second experiment represents three volcanic belts composed of basalt blocks along the width of PVC sheet, on white layer of sand and in between the two (red and blue) layers of sand left of the rigid backstop. The volcanic belts were placed 15, 30 and 45 cm from the backstop. The belts were 20 cm width and approximately 1 cm high. The bulk of the white layer had 180 grams along 60 cm length of the PVC sheet with 20 cm width and 1.5 cm high. The red and blue layers surrounding volcanic belts have had both 180 grams each with 1.6 high respectively. The dip of the rigid backstop, same as previous experiment was set to 60°, along with 0° dip of "subducting oceanic plate". The motion of the PVD sheet was set to 0.01 cm/s and the experiment was captured every 30 seconds by a digital single-lens reflex (SLR) camera.

4.3 Results

Results of the experiments are shown in Figs. 11, 12,13 and described in detail below.

4.3.1 Experiment 1

In the beginning of the experiment 1 (Fig. 13a), as the seamount approaches the trench, the accretionary wedge already deforms by internal thrusting and a series of in-sequence thrust planes develops to shorten and thicken the wedge to reach a critical taper. The first key event is observed when the seamount approaches and starts to mechanically interact with the wedge (Fig. 13b). At this time, a zone of intense shear deformation develops along the seamount/wedge interface (Fig. 13b). The material from accretionary wedge starts to "climb" over the landward side of the seamount (Fig. 13c) and, with continuous movement of the seamount towards the backstop, the sand from accretionary wedge interacts and mixes with the seamount-derived blocks to form mélange (Fig.13d). The mélange exhibits a block-in-matrix fabric and forms a thin, landward-dipping zone enveloping the seamount (Fig.13d).

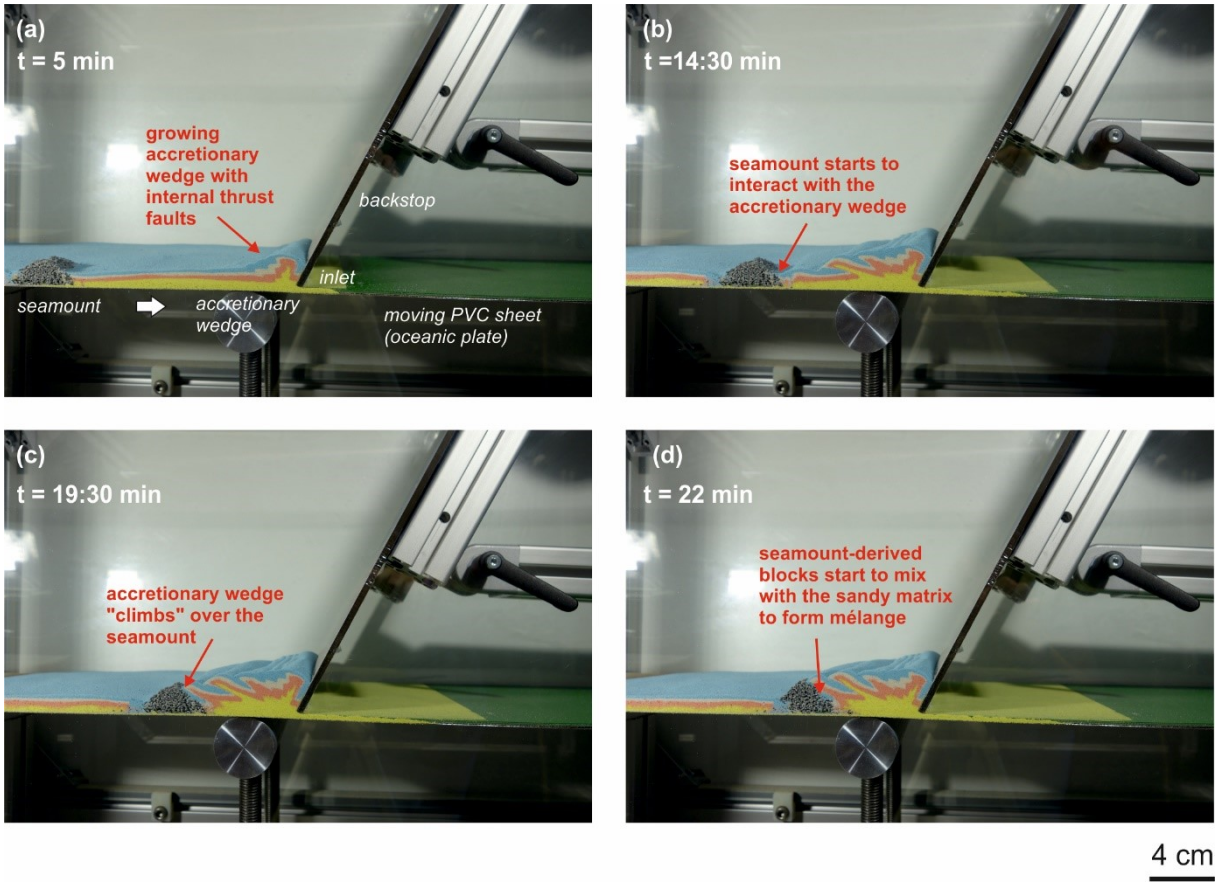

Figure 13. Results of the experiment 1 from a time interval of 5–22 minutes. For more information see text.

The second key event is at 24th minute of the experiment when the trenchward side of the seamount is under intense shear deformation (Fig. 14a). The deformation on the trenchward side of the seamount, caused by the progressive movement of the PVC sheet ("oceanic plate"), activates new thrust surface (Fig. 14b) while the accretionary wedge between the seamount and the backstop thickens significantly as compared to the time interval before the seamount–wedge interaction (Fig. 14b). From time t = 24 min to time t = 28 min, intense shear deformation on the oceanward side of the seamount creates a new landward-dipping thrust fault (Fig. 14c). After that, the accretion and deformation of the material is transferred to the oceanward side of the seamount forming additional in-sequence thrusts within a "new" accretionary wedge that establishes a critical taper. In contrast, the rear part of the "original" wedge (between the seamount and the backstop) is locked and forms a sort of plateau with corrugated surface until the end of experiment at time t = 41 min (Fig. 14d).

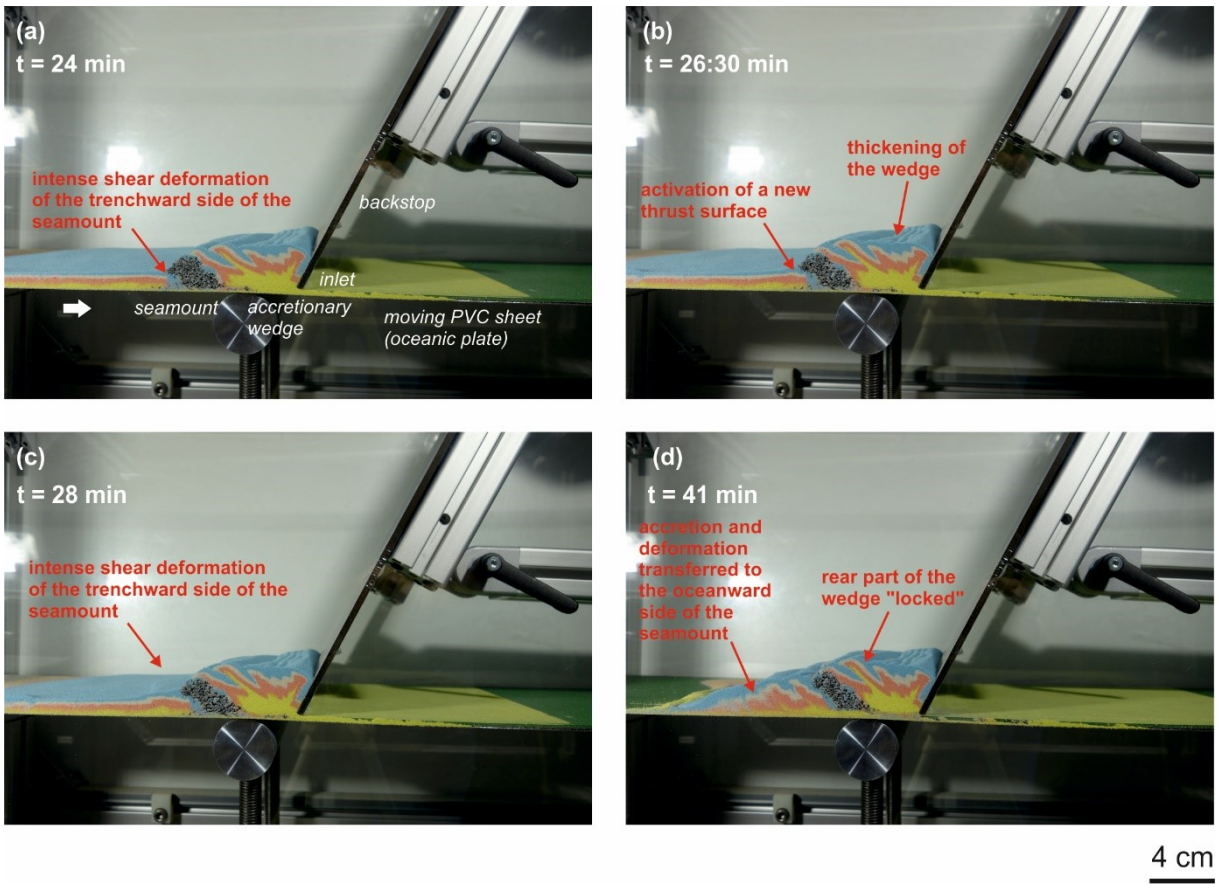

Figure 14. Results of the experiment 1 from a time interval of 24–41 minutes. For more information see text.

4.3.2 Experiment 2

At the beginning of the experiment 2 (Fig. 15a) a small accretionary prism is formed at

the base of backstop and by the 13th minute the first volcanic ridge starts to interact with the growing accretionary wedge. The accretionary wedge deforms internally and a series of thrust planes shorten and thicken the wedge to reach the critical taper.

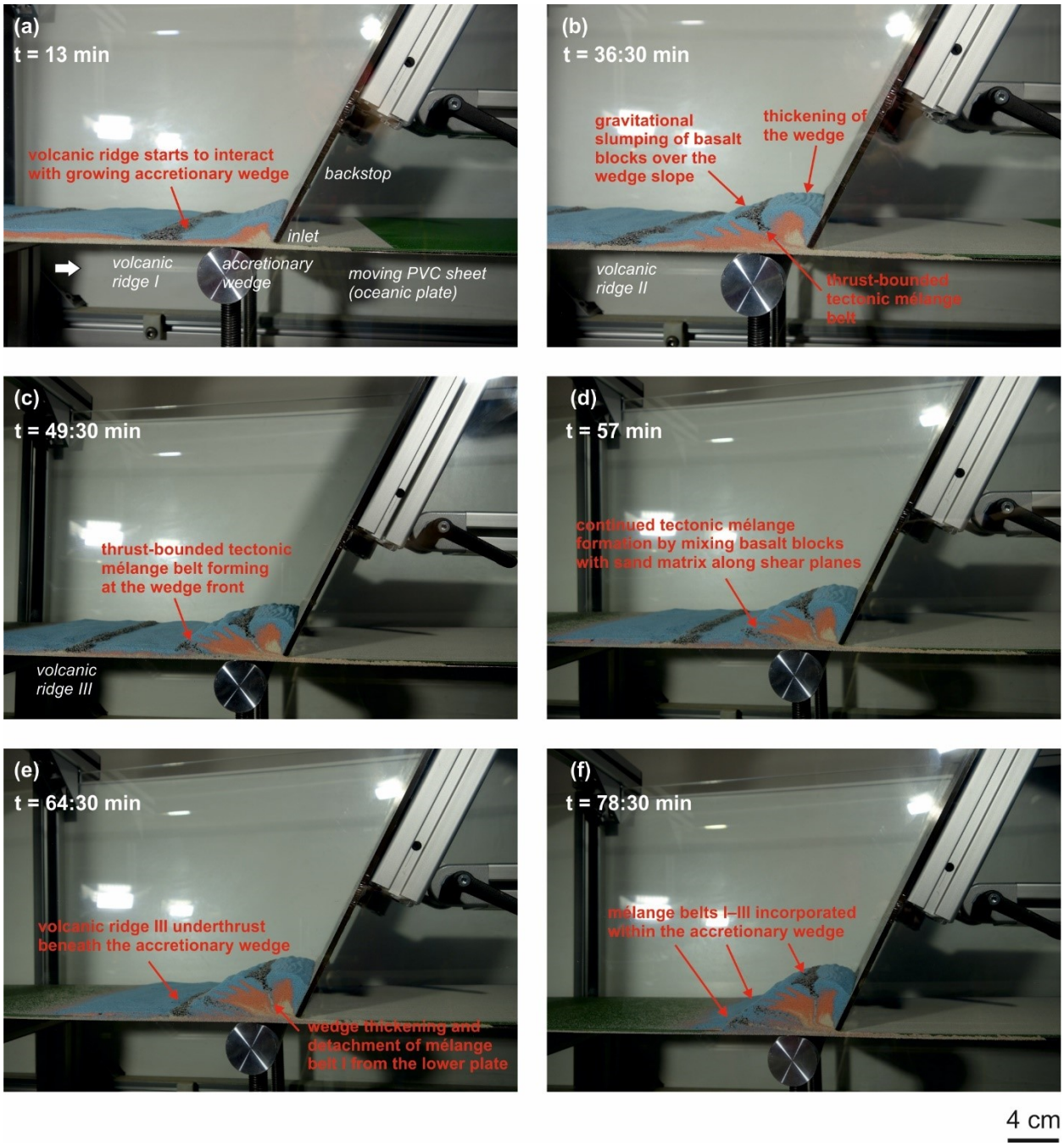

Figure 15. Results of the experiment 2 from a time interval of 13 - 78:30 minutes. For more information see text.

As the subduction continues (Fig. 15b), the first volcanic ridge (I) is incorporated into the wedge creating thrust-bounded tectonic mélange belt within the wedge. The landward side of the wedge, separated by the mélange belt, thickens together with accreted material. The seaward side

is pushed by off-scrapped material from the moving PVC sheet, continuously forming new fold-and-thrust belts. The basalt blocks in the near-surface part of the volcanic ridge I then start to form gravitational slumps over the wedge slope. The later impingement of the second volcanic ridge (II) into the further growing accretionary prism leads to formation of another thrust-bounded tectonic mélange belt at the wedge front (Fig. 15c). The overall thickening and growth of the accretionary prism continues while the newly formed mélange is being underthrust beneath the accretionary wedge and detached from the subducting lower plate (Fig. 15c). With continuing accretion and deformation of the volcanic ridge II, tectonic mélanges are formed by mixing the basalt blocks with the sandy matrix along planes of intense shear deformation (Fig. 15d). Last, the volcanic ridge III is underthrust at the base of the still expanding accretionary wedge (Fig. 15e). The accretionary prism enlarges and thickens with continuously emplaced sand and volcanic ridges whilst the mélanges I and II are being progressively more detached and displaced from the lower plate. In the very final stage of the experiment, all three volcanic belts are incorporated within the accretion prism, at the end of the experiment at time t=78:30 min (Fig. 15f).

The implications of both experiments are discussed in the Chapter below.

5 Discussion

The aim of the first part of the thesis was to describe the architecture of subduction zones (Fig. 2) and the complexity of subduction zone processes and to discuss various experimental approaches to simulate these processes. As it was discussed in chapters above, the oceanic plate carries sedimentary and magmatic material on its way to the convergent margin, where the oceanic material from the lower (oceanic) plate and the terrigenous material from the overriding plate are mixed in accretionary prisms. Formation of the subduction mélanges is a common process, and it is the main focus of this thesis.

One of the most effective mechanism for mixing of the oceanic and terrigenous material is subduction of seamounts that form high elevations on the seafloor surrounded by thick debris aprons (e.g., (Clarke et al., 2018)). These elevations may, however, also be covered by pelagic material. The high topography makes the entering of the seamount into the subduction zone rather difficult (e.g., (Ding and Lin, 2016; Watts et al., 2010)). Seamount subduction may also produce disrupted Ocean Plate Stratigraphy, i.e., the so-called OPS, mélanges that form due to tectonic erosion of seamounts inside the accretionary prism (Fig. 6). A great example of the basalt-bearing OPS mélanges was described by (Hajná et al., 2014; Hajná et al., 2013) in the Neoproterozoic to early Cambrian Blovice accretionary complex in the Bohemian Massif (the analog model presented in this thesis attempted to also simulate formation of these mélanges).

The second pard of the thesis aimed to describe some of the mechanisms that may produce the OPS mélanges using analog experiments and to provide overview of analog models, along with common use of appropriate material and proper scaling, of development of accretionary wedges.

The analog modeling contributes significantly to studies in plate tectonics and structural geology. Numerous experiments were successfully conducted using different experimental devices especially to study evolution and deformation of accretionary prisms (Fig. 14; accretion and underplating, surface erosion, salt diapirism, etc.). Many studies focused on subduction of seamounts entering the subduction zone, with variety of possible mechanical properties, structure, and arrays of seamounts (e.g.,(Dominguez et al., 1998; Dominguez et al., 2000; Wang et al., 2021)).

The third part of the thesis involved new experiments. In contrast to previous models that focused on the deformation of the accretionary wedge due to seamount subduction ((Clarke et al., 2018; Dominguez et al., 2000), etc.), the main goal of our experiments was to simulate the

formation of basalt-bearing mélanges. Our model seamount was composed of blocks of basalt as an analog of thick debris aprons in moat basin around seamounts (Clarke et al., 2018) rather than solid gypsum usually used in most seamount models. Such a fragmented seamount was able not only to deform within the accretionary wedge but also to create mélange structures (Figs. 13-15), unlike developing a fan fault system as in the gypsum seamount experiments. In a similar way, the three volcanic belts were also made of the basalt blocks instead of solid material (Fig. 15). Using basalt blocks was designed to simulate the mélange deformation in accretionary wedges, perhaps closer to natural examples of weathered fragmented seamounts.

As every analog model, the experiments presented in this thesis should be considered as a greatly simplified reproduction of complex natural processes. The boundary conditions, geometry of the model and rheology of the used analog materials are all simplified as compared to nature. Moreover, the apparatus does not allow to involve fluids in the experiment, which are a key feature of subduction zones, increasing pore pressure and thus reducing the effective stress, hydrating mineral phases, and lubricating fault planes. Another important limitation of the models lies within the fact that the seamount and the volcanic belts were composed of smaller dry blocks to model the formation of mélanges. In nature, seamounts are composed of a solid core (coherent basaltic rock) that is surrounded by thick accumulations of disintegrated, loose blocks (talus) with the space in between filled with water or deep-sea sediment.

On the other hand, the experimental models described in the previous chapter indicated several important processes that may occur during incorporation of single seamounts (Fig. 13, Fig. 14) and multiple volcanic belts into accretionary complexes (Fig. 15). The main outcomes of the experiments are as follows:

First, the experiment showed that it is the loose blocks rimming the seamounts that will be preferentially incorporated into mélanges. Especially the landward side of the seamounts is the potential site from where the blocks may be dragged by shear and mixed with the terrigenous sand (Fig. 13d).

Second, it was demonstrated that from the early stages of seamount/wedge collision, the mechanical interaction of the block-composed seamount with the sandy accretionary wedge increased the critical taper of the prism (Fig. 14a) and, in turn, also led to formation of a “plateau” in the rear part of the wedge at the end of experiment. The plateau had a significantly corrugated surface (Fig 12b).

Third, at the same time, the accretion and deformation continued on the oceanward side of the seamount with propagation of new in-sequence thrust faults towards the trench (Fig. 14d). In this scenario, the seamount within the wedge behaves as a new, second-order backstop,

supporting thrust fault propagation until the end of experiment. It is also important to note that during the course of the seamount/wedge interaction, the increased wedge taper produced massive slumping of material from the accretionary prism and partly also of basalt blocks from the seaward side of the seamount. The seamount subduction thus clearly triggers significant mass-wasting processes along the wedge surface and transport of material towards the trench to form the trench-fill deposits.

Fourth, as a result of impingement of the seamount into the accretionary wedge and formation of the "second-order" backstop, the wedge was mechanically separated into two parts, a flat rear part, and a frontal wedge (Fig. 14d). The thrust faulting within both parts of the wedge created linear (trench-parallel) piggyback basins on the upper wedge surface, where a significant amount of arc-derived sediment may be trapped during subduction.

Fifth, more complex structures form when several seamount ridges/belts interact with the wedge (Fig. 15). The accretion of the seamount belt results in several slumps of basaltic blocks on the surface of the accretionary prism and possibly form sedimentary mélanges (Fig. 15b) which cloud be again later reincorporated into the trench. The seamount (volcanic) ridges each form tectonic mélange belts within the accretionary wedge system (Fig. 15e) and with further growth and thickening of the prism the volcanic belts are underthrust and detached from the bottom layer (Fig. 15f).

Although the presented experimental model was greatly simplified, it showed the complexity of the seamount–wedge interactions and, most importantly, pointed to several promising directions for future research. The next stage of analog experiments could involve (1) more realistic shapes of the seamounts in terms of their size (scale), slope angles, and internal structure, (2) involvement of blocks of different composition and density that form the Ocean Plate Stratigraphy (e.g., limestones and cherts), (3) protracted successive subduction of several linear seamount chains, and (4) various geometries of the subduction zone and backstop angle. Furthermore, the experimental models should always be validated by comparison with field observations from natural examples. This may be done by a detailed survey of exiting data on recent seamounts (to characterize their geometry and internal structure) and by detailed field studies of ancient basalt-bearing mélanges.

6 Conclusions

The main conclusions of this Bachelor (Bc.) thesis are as follows:

(1) The thesis demonstrated the complexity of subduction zones and their internal structure and evolution.

(2) A review of existing analog experiments showed that many processes may be successfully reproduced in the laboratory, however, many processes related to interaction of oceanic and terrigenous material remain largely unexplored.

(3) It is the loose blocks surrounding the seamount, that are eventually incorporated into mélanges in seamount/wedge interaction

(4) The simple experimental model of seamount subduction showed that the collision between the accretionary wedge of sandy composition and the seamount composed of blocks first increased critical taper of the wedge.

(5) The increase of the critical taper of the accretionary wedge due to the change in physical properties led to formation of a “plateau” in the rear part of the wedge.

(6) The accretion of oceanic material is associated with extensive mass-wasting along the wedge surface and continues on the oceanward side of the accreted seamount.

(7) The incorporated seamount behaves as a new “second-order” backstop, mechanically separating the accretionary wedge into two parts, the rear “locked” part and a frontal wedge.

(8) The arc-derived sediment may be trapped by the trench-parallel piggyback basins formed by the thrusting on the top of the wedge.

(9) The smaller seamount structures such as volcanic belts are easier incorporated into accretionary wedge and thus more likely to form tectonic mélanges.

(10) The tectonic mélanges are underthrust under accretionary wedge and with continuous growing and thickening of the prism the mélanges are detached from bottom layer.

(11) As a direction of future research, the next stages of analog modeling of the

subduction zone with seamount/accretionary wedge interaction will be performed with more detailed and complicated setting (scaling properties of seamount, material similar to the Ocean Plate Stratigraphy, more complex multiple seamounts entering subduction zone, various angles of the backstop and the basal dip, etc.).

7 References

Agard, P., Plunder, A., Angiboust, S., Bonnet, G. and Ruh, J., 2018. The subduction plate interface: rock record and mechanical coupling (from long to short timescales). Lithos, 320-321: 537–566.

Arndt, N., 2011. MORB. In: M. Gargaud, R. Amils, J.C. Quintanilla, H.J. Cleaves, W.M. Irvine, D.L. Pinti and M. Viso (Editors), Encyclopedia of Astrobiology. Springer Berlin Heidelberg, Berlin, Heidelberg, pp. 1097-1097.

Buiter, S.J.H., 2012. A review of brittle compressional wedge models. Tectonophysics, 530-531: 1-17.

Cawood, P., Kröner, A., Collins, W., Kusky, T., Mooney, W. and Windley, B., 2009. Accretionary orogens through Earth history, pp. 1-36.

Clarke, A.P., Vannucchi, P. and Morgan, J., 2018. Seamount chain-subduction zone interactions: Implications for accretionary and erosive subduction zone behavior. Geology, 46(4): 367-370.

Clift, P., 2004. Controls on tectonic accretion versus erosion in subduction zones: Implications for the origin and recycling of the continental crust. Reviews of Geophysics, 42(2).

Clift, P. and Vannucchi, P., 2004. Controls on tectonic accretion versus erosion in subduction zones: Implications for the origin and recycling of the continental crust. Reviews of Geophysics, 42(2): RG2001.

Clift, P.D., MacLeod, C.J., Tappin, D.R., Wright, D.J. and Bloomer, S.H., 1998. Tectonic controls on sedimentation and diagenesis in the Tonga Trench and forearc, southwest Pacific. GSA Bulletin, 110(4): 483-496.

Cloetingh, S., Wortel, R. and Vlaar, N.J., 1989. On the initiation of subduction zones. Pure and Applied Geophysics, 129(1-2): 7-25.

Cloos, M., 1993a. Lithospheric buoyancy and collisional orogenesis- subduction of oceanic plateaus, continental margins, island arcs, spreading ridges, and seamounts. Geological Society of America Bulletin, 105(6): 715-737.

Cloos, M., 1993b. Lithospheric buoyancy and collisional orogenesis: subduction of oceanic plateaus, continental margins, island arcs, spreading ridges, and seamounts. Geological Society of America Bulletin, 105: 715–737.

Cloos, M. and Shreve, R.L., 1988a. Subduction-channel model of prism accretion, melange formation, sediment subduction, and subduction erosion at convergent plate margins .1. Background and description. Pure and Applied Geophysics, 128(3-4): 455-500.

Cloos, M. and Shreve, R.L., 1988b. Subduction-channel model of prism accretion, melange formation, sediment subduction, and subduction erosion at convergent plate margins .2. Implications and disscusion. Pure and Applied Geophysics, 128(3-4): 501-545.

Cloos, M. and Shreve, R.L., 1996. Shear-zone thickness and the seismicity of Chilean- and Marianas-type subduction zones. Geology, 24(2): 107-110.

Cowan, D.S. and Silling, R.M., 1978. Dynamic, scaled model of accretion at trenches and its implications for tectonic evolution of subduction complexes Journal of Geophysical Research, 83(NB11): 5389-5396.

Dickinson, W.R., 1975. Potash–dept relations (K–h) in continental margin and intra-oceanic magmatic arcs. Geology, 3: 53–56.

Ding, M. and Lin, J., 2016. Deformation and faulting of subduction overriding plate caused by a subducted seamount. Geophysical Research Letters, 43(17): 8936-8944.

Doglioni, C., Carminati, E., Cuffaro, M. and Scrocca, D., 2007. Subduction kinematics and dynamic constraints. Earth-Science Reviews, 83(3-4): 125-175.

Dominguez, S., Lallemand, S.E., Malavieille, J. and Von Huene, R., 1998. Upper plate deformation associated with seamount subduction. Tectonophysics, 293(3-4): 207-224.
Dominguez, S., Malavieille, J. and Lallemand, S.E., 2000. Deformation of accretionary wedges in response to seamount subduction: Insights from sandbox experiments. Tectonics, 19(1): 182-196.
Ducea, M.N., Kidder, S., Chesley, J.T. and Saleeby, J.B., 2009. Tectonic underplating of trench sediments beneath magmatic arcs: the central California example. International Geology Review, 51(1): 1–26.
Ducea, M.N., Saleeby, J.B. and Bergantz, G., 2015. The architecture, chemistry, and evolution of continental magmatic arcs. Annual Review of Earth and Planetary Sciences, 43(1): 299-331.
Festa, A., Pini, G.A., Dilek, Y. and Codegone, G., 2010. Melanges and melange-forming processes: a historical overview and new concepts. International Geology Review, 52(10-12): 1040-1105.
Festa, A., Pini, G.A., Ogata, K. and Dilek, Y., 2019. Diagnostic features and field-criteria in recognition of tectonic, sedimentary and diapiric mélanges in orogenic belts and exhumed subduction-accretion complexes. Gondwana Research, 74: 7–30.
Forsyth, D. and Uyeda, S., 1975. On the relative importance of the driving forces of plate motion. Geophysical Journal of the Astronomical Society, 43: 163–200.
Graveleau, F., Malavieille, J. and Dominguez, S., 2012. Experimental modelling of orogenic wedges: A review. Tectonophysics, 538-540: 1-66.
Gutscher, M.A., Kukowski, N., Malavieille, J. and Lallemand, S., 1998. Material transfer in accretionary wedges from analysis of a systematic series of analog experiments. Journal of Structural Geology, 20(4): 407-416.
Hajná, J., Žák, J. and Kachlík, V., 2014. Growth of accretionary wedges and pulsed ophiolitic melange formation by successive subduction of trench-parallel volcanic elevations. Terra Nova, 26(4): 322–329.
Hajná, J., Žák, J., Kachlík, V., Dörr, W. and Gerdes, A., 2013. Neoproterozoic to early Cambrian Franciscan-type mélanges in the Teplá–Barrandian unit, Bohemian Massif: evidence of modern-style accretionary processes along the Cadomian active margin of Gondwana? Precambrian Research, 224: 653–670.
Harper, J.F., 1975. Driving forces of plate tectonics. Geophysical Journal of the Royal Astronomical Society, 40(3): 465-474.
Hickey, R.L. and Frey, F.A., 1982. Geochemical characteristics of boninite series volcanics: implications for their source. Geochimica et Cosmochimica Acta, 46: 2099–2115.
Huangfu, P., Wang, Y.J., Li, Z.H., Fan, W.M. and Zhang, Y., 2016. Effects of Crustal Eclogitization on Plate Subduction/Collision Dynamics: Implications for India-Asia Collision. Journal of Earth Science, 27(5): 727-739.
Hühnerbach, V., Masson, D.G., Bohrmann, G., Bull, J.M. and Weinrebe, W., 2005. Deformation and submarine landsliding caused by seamount subduction beneath the Costa Rica continental margin — new insights from high-resolution sidescan sonar data. Geological Society, London, Special Publications, 244(1): 195-205.
Hüneke, H. and Henrich, R., 2011. Pelagic Sedimentation in Modern and Ancient Oceans. Developments in Sedimentology, 63: 216–295.
Chen, L., Wang, X., Liang, X.F., Wan, B. and Liu, L.J., 2020. Subduction tectonics vs. Plume tectonics-Discussion on driving forces for plate motion. Science China-Earth Sciences, 63(3): 315-328.
Jarrard, R.D., 1986. Relations among subduction parameters. Reviews of Geophysics, 24(2): 217-284.
Kearey, P., Klepeis, K.A. and Vine, F.J., 2009. Global Tectonics. Wiley.

Kusky, T., Wang, J.P., Wang, L., Huang, B., Ning, W.B., Fu, D., Peng, H.T., Deng, H., Polat, A., Zhong, Y.T. and Shi, G.Z., 2020. Melanges through time: Life cycle of the world's largest Archean melange compared with Mesozoic and Paleozoic subduction-accretion-collision melanges. Earth-Science Reviews, 209.

Kusky, T.M., Windley, B.F., Safonova, I., Wakita, K., Wakabayashi, J., Polat, A. and Santosh, M., 2013. Recognition of ocean plate stratigraphy in accretionary orogens through Earth history: a record of 3.8 billion years of sea floor spreading, subduction, and accretion. Gondwana Research, 24(2): 501–547.

Lallemand, S. and Funiciello, F., 2009. Subduction Zone Geodynamics. Subduction Zone Geodynamics edited by Serge Lallemand and Francesca Funiciello. Berlin: Springer, 2009. ISBN: 978-3-540-87974-9.

Lallemand, S., Heuret, A., Faccenna, C. and Funiciello, F., 2008. Subduction dynamics as revealed by trench migration. Tectonics, 27(3): 15.

Maruyama, S. and Safonova, I., 2019. Orogeny and mantle dynamics: role of tectonic erosion and second continent in the mantle transition zone.

Matsuda, T. and Isozaki, Y., 1991. Well-documented travel history of Mesozoic pelagic chert in Japan: from remote ocean to subduction zone. Tectonics, 10: 475–499.

Morley, C., 1988. Out-of-Sequence Thrusts. Tectonics, 7.

Noda, A., Koge, H., Yamada, Y., Miyakawa, A. and Ashi, J., 2020. Subduction of trench-fill sediments beneath an accretionary wedge: Insights from sandbox analogue experiments. Geosphere, 16(4): 1664-1679.

Ogata, K., Festa, A., Pini, G.A. and Alonso, J.L., 2020. Submarine landslide deposits in orogenic belts: olistostromes and sedimentary mélanges. Geophysical Monograph, 246: 3–26.

Raymond, L.A., 2019. Origin of Melanges of the Franciscan Complex, Diablo Range and Northern California: An Analysis and Review. Geosciences, 9(8).

Reber, J.E., Cooke, M.L. and Dooley, T.P., 2020. What model material to use? A Review on rock analogs for structural geology and tectonics. Earth-Science Reviews, 202: 103107.

Ruh, J.B., Sallares, V., Ranero, C.R. and Gerya, T., 2016. Crustal deformation dynamics and stress evolution during seamount subduction: High-resolution 3-D numerical modeling. Journal of Geophysical Research-Solid Earth, 121(9): 6880-6902.

Safonova, I., Maruyama, S., Kojima, S., Komiya, T., Krivonogov, S. and Koshida, K., 2016. Recognizing OIB and MORB in accretionary complexes: a new approach based on ocean plate stratigraphy, petrology and geochemistry. Gondwana Research, 33: 92–114.

Santosh, M., 2010. A synopsis of recent conceptual models on supercontinent tectonics in relation to mantle dynamics, life evolution and surface environment. Journal of Geodynamics, 50(3–4): 116–133.

Schellart, W.P. and Strak, V., 2016. A review of analogue modelling of geodynamic processes: Approaches, scaling, materials and quantification, with an application to subduction experiments. Journal of Geodynamics, 100: 7-32.

Silver, E.A., Ellis, M.J., Breen, N.A. and Shipley, T.H., 1985. Comments on the growth of accretionary wedges. Geology, 13: 6–9.

Simpson, G.D.H., 2010. Formation of accretionary prisms influenced by sediment subduction and supplied by sediments from adjacent continents. Geology, 38(2): 131-134.

Stern, C.R., 2011. Subduction erosion: Rates, mechanisms, and its role in arc magmatism and the evolution of the continental crust and mantle. Gondwana Research, 20(2-3): 284-308.

Stern, R.J., 2002. Subduction zones. Reviews of Geophysics, 40(4).

Stern, R.J., 2004. Subduction initiation: spontaneous and induced. Earth and Planetary Science Letters, 226(3-4): 275-292.

Stern, R.J. and Gerya, T., 2018. Subduction initiation in nature and models: A review. Tectonophysics, 746: 173-198.

Suetsugu, D., Steinberger, B. and Kogiso, T., 2013. Mantle Plumes and Hotspots☆, Reference Module in Earth Systems and Environmental Sciences. Elsevier.
Uyeda, S. and Kanamori, H., 1979. Back-arc opening and the mode of subduction. Journal of Geophysical Research, 84(B3): 1049.
von Huene, R. and Scholl, D.W., 1991. Observations at convergent margins concerning sediment subduction, subduction erosion, and the growth of continental crust. Reviews of Geophysics, 279–316.
Wada, I., Wang, K.L., He, J.G. and Hyndman, R.D., 2008. Weakening of the subduction interface and its effects on surface heat flow, slab dehydration, and mantle wedge serpentinization. Journal of Geophysical Research-Solid Earth, 113(B4): 15.
Wakita, K., 2015. OPS mélange: a new term for mélanges of convergent margins of the world. International Geology Review, 57(5–8): 529–539.
Wang, C., Ding, W., Schellart, W.P., Li, J., Dong, C., Fang, Y., Hao, T. and Tong, Z., 2021. Effects of multi-seamount subduction on accretionary wedge deformation: Insights from analogue modelling. Journal of Geodynamics, 145: 101842.
Wang, K.L. and Bilek, S.L., 2011. Do subducting seamounts generate or stop large earthquakes? Geology, 39(9): 819-822.
Watts, A.B., Koppers, A.A.P. and Robinson, D.P., 2010. Seamount Subduction and Earthquakes. Oceanography, 23(1): 166-173.